Mobility and carrier density in nanoporous indium tin oxide films

A. Gondorf, M. Geller, J. Weißbon, and A. Lorke
Fakultät für Physik and CeNIDE, Universität Duisburg-Essen, D-47048 Duisburg, Germany

M. Inhester, A. Prodi-Schwab, and D. Adam
Evonik Degussa GmbH, D-45772 Marl, Germany

(Received 7 October 2010; revised manuscript received 31 January 2011; published 10 June 2011)

The charge-carrier concentration and mobility of various nanoporous indium tin oxide films have been studied by Hall measurements and optical spectroscopy. The carrier density obtained by Hall measurements is found to be significantly lower than that derived from optical spectroscopy. The results of these complementary measurement techniques thus support recent theoretical work on granular conducting layers by Kharitonov and Efetov [Phys. Rev. B **77**, 045116 (2008)], which predicts that the Hall carrier concentration n of such a system is reduced by a geometrical factor. As expected, the mobility inside the particles, derived from optical transmission spectra ($22-35\ \frac{\mathrm{cm}^2}{\mathrm{Vs}}$), is much higher than the macroscopic Hall mobility ($0.12-0.7\ \frac{\mathrm{cm}^2}{\mathrm{Vs}}$).

DOI: 10.1103/PhysRevB.83.212201 PACS number(s): 73.63.−b, 73.22.−f, 78.67.Bf

In recent years, indium tin oxide (ITO) has become an indispensable material for a range of electronic devices. The very high doping of indium oxide with tin leads to carrier densities[1–3] of $1-10\times10^{20}\,\mathrm{cm}^{-3}$ or even above $10\times10^{20}\,\mathrm{cm}^{-3}$. At these high doping levels, the Mott limit[4] is exceeded, making ITO a degenerate semiconductor with metallic properties. The plasma frequency at these carrier concentrations is in the infrared, so that light of lower frequencies is reflected and light of higher frequencies is transmitted. On the other hand, the optical band-gap energy of ITO is about 3.5 eV,[5] so that interband absorption is possible only in the ultraviolet. This results in light being transmitted in the entire visible range. The combination of these properties makes ITO a well-suited material for transparent electrodes used, for example, in LCD displays, touch screens, and thin-film solar cells.

In the conventional ITO-coating process, ITO is evaporated or sputtered on glass substrates in a vacuum chamber. An interesting alternative to realize transparent, conducting films is the use of dispersions containing ITO nanoparticles.[6] Such films can in principle be realized without the use of vacuum techniques or high-temperature processes, so that roll-to-roll-fabrication on flexible polymer material becomes possible. Furthermore, ITO nanoparticle dispersions can easily be patterned using inexpensive printing techniques.

In granular nanoscale materials the simple application of macroscopic characterization tools may be questionable. For example, derivation of the Hall and van der Pauw formula assumes that the sample is homogeneous and – in the mathematical sense – simply connected.[7] Both assumptions, however, are not fulfilled for porous materials such as the ITO layers under consideration here. For optical properties and nanoscale porosity (wavelength $\gg$ particle size), effective medium theories have been developed, such as the Bruggeman formula.[8] However, as Kharitonov and Efetov have pointed out, up to the year 2008, "Hall transport in such granular materials has not been addressed theoretically before, neither in the insulating nor the metallic regimes."[9] Also, little experimental work on the Hall effect in nanoparticle layers was available.[10–13] As the combination of Hall measurements and optical spectroscopy has been successfully used to characterize electronic properties of thin films of microcrystalline transparent conductors,[14–16] it offers the opportunity to test the recent theoretical work on nanoscale granular conductors.[9]

Here we investigate conducting granular layers consisting of ITO particles with diameters of about 20 nm. The particles have been fabricated in a liquid-phase precipitation process under varying temperatures and precipitation velocities. Variation of these parameters leads to changes in the charge-carrier concentration. The particles were dispersed in ethanol (mass fraction of the ITO particles was about 25−40%) and printed on glass substrates. They were subsequently heated at 500 °C under ambient conditions and in a second step at 300 °C in a 95% N_2 + 5% H_2 atmosphere. The layer thickness is 800 nm for the thinnest and 950 nm for the thickest sample, as determined from our measurements (see below).

I. OPTICAL SPECTROSCOPY

Figure 1 shows a scanning electron microscopy (SEM) image of an ITO-nanoparticle layer. In order to determine the thickness d and the filling factor f of the ITO nanoparticle films, we perform reflectance measurements in a Fourier transform infrared (FTIR) spectrometer. In Fig. 2 the reflection spectrum of an ITO nanoparticle layer in the energy range between 1.35 and 2.15 eV, corresponding to a wavelength between 580 and 920 nm, is shown. The spectrum shows typical Fabry-Perot interference effects with an energy difference ΔE between two neighboring reflection minima. ΔI is the difference between the detected intensity at a maximum (constructive interference) and a minimum (destructive interference). Starting from a three-medium model with the first layer being air, the second layer ITO nanoparticles, and the third layer the glass substrate (refractive index n_G), we calculate n_{eff}:[17]

$$\Delta I = \mathrm{R}_{\mathrm{max}} - \mathrm{R}_{\mathrm{min}} = \left(\frac{n_G - n_{\mathrm{eff}}^2}{n_G + n_{\mathrm{eff}}^2}\right)^2 - \left(\frac{1-n_G}{1+n_G}\right)^2. \quad (1)$$

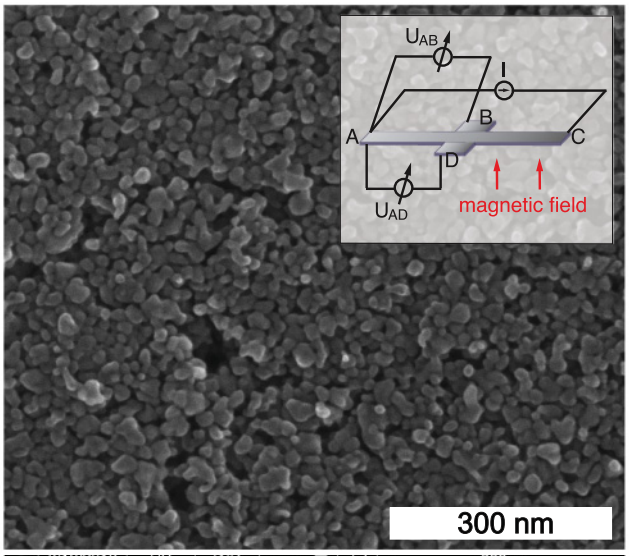

FIG. 1. (Color online) SEM image of an ITO nanoparticle layer. The inset shows the measurement geometry.

Because in the energy range of interest (1.5 − 2.0 eV) the refractive index of ITO[14] varies less than 5% for a carrier concentration below 4.9×10^{20} cm^{-3}, we can use a constant n_{eff} to obtain the layer thickness from

$$d = \frac{hc}{2n_{\text{eff}}\Delta E}. \tag{2}$$

From the Bruggeman formula,[8]

$$f\frac{\varepsilon_{ITO}(\omega) - \varepsilon_{\text{eff}}(\omega)}{\varepsilon_{ITO}(\omega) + 2_{\text{eff}}(\omega)} + (1-f)\frac{\varepsilon_0 - \varepsilon_{\text{eff}}(\omega)}{\varepsilon_0 + 2\varepsilon_{\text{eff}}(\omega)} = 0, \tag{3}$$

and using $\varepsilon_{\text{eff}} = n_{\text{eff}}^2$ it is possible to calculate the volume fraction occupied by ITO nanoparticles (filling factor f). The resulting values for thickness and filling factor are summarized in Table I.

TABLE I. Sample parameters as determined by Hall measurements and optical spectroscopy on different ITO layer samples.

Sample number	d nm	f	n_{Hall}	n_{opt}	μ_{Hall}	μ_{opt}
			10^{20} cm^{-3}		cm^2/Vs	
1	950	0.80	2.1	4.3	0.66	35
2	870	0.80	2.1	3.9	0.33	32
3	800	0.78	2.3	3.9	0.32	30
4	800	0.78	2.2	3.9	0.44	29
5	800	0.78	1.8	3.4	0.72	27
6	850	0.79	1.7	2.8	0.12	22
7	810	0.76	3.0	3.5	0.19	26
8	850	0.82	3.4	4.3	0.19	32
9	820	0.79	1.8	3.5	0.20	30

In Fig. 3, a transmission and reflection spectrum for a much larger energy range (0.4 − 2.5 eV), which includes the ITO plasma edge, is shown. Above the plasma edge energy, the transmission is as high as 85%, which demonstrates the high quality of the printed film. Below the plasma edge energy, the transmission is near zero.

To calculate the reflection and transmission of the ITO nanoparticle layers we follow the approach by Ederth *et al.*[6] The dielectric function inside the individual nanoparticles can be calculated using the free-electron gas model:

$$\varepsilon_{ITO}(\omega) = \varepsilon_\infty - \frac{\omega_p^2}{\omega \cdot \left(\omega + \frac{i}{\tau_{\text{IIS}}}\right)}, \tag{4}$$

with ω being the frequency of the light, ω_p the plasma frequency, and i/τ_{IIS} the damping. We use $\varepsilon_\infty = 4$ in our calculations.[6] In heavily doped ITO the electrons are scattered by ionized dopant atoms. The relaxation time τ_{IIS} therefore can be found considering ionized impurity scattering (IIS).[2,18] It is given by

$$\tau_{\text{IIS}}(\omega) = \tau_0 \left(\frac{\omega_p}{\sqrt{\varepsilon_\infty}}\right)^{-\frac{3}{2}} \omega^{\frac{3}{2}}. \tag{5}$$

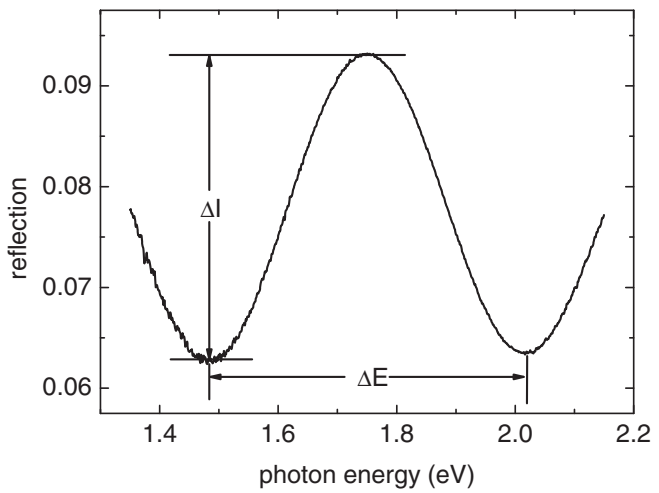

FIG. 2. Reflection spectrum of sample 9 in the optical range. The Fabry-Perot oscillations are used to determine filling factor f and thickness d of the ITO layer.

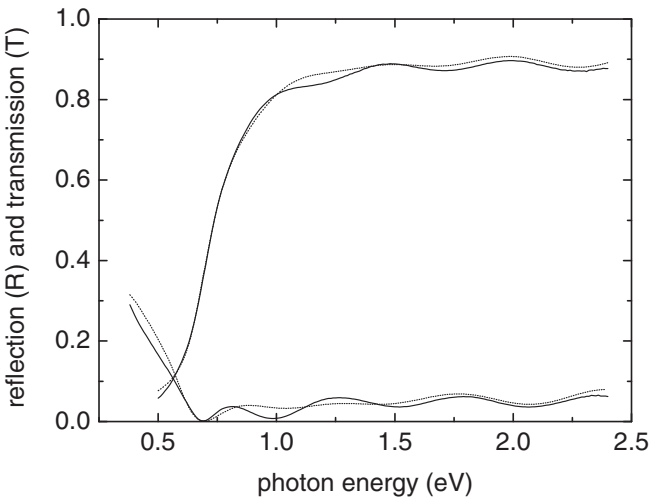

FIG. 3. Transmission and reflection spectrum of sample 9. Solid lines: experimental data, dotted lines: calculated transmission and reflection.

By inserting Eqs. (4) and (5) into Eq. (3) (taking the parameters d and f from the reflection measurements) we calculate the wavelength-dependent effective dielectric function of the ITO nanoparticle layers.

We can fit our experimental data (Fig. 3, solid line) with the now-given $\varepsilon_{\text{eff}}(\omega)$ using the three-layer model above. An effective electron mass $m_e = 0.3m_0$ is used,[1,18] and τ_0 and ω_p are taken as fit parameters. Both transmission and reflection show good agreement with the calculations. The carrier density n_{opt} and mobility μ_{opt} of the ITO particles are then calculated by

$$n_{opt} = \frac{\omega_p^2 m_e \varepsilon_0}{e^2} \quad \text{and} \quad \mu_{opt} = \frac{e\tau_0}{m_e}, \tag{6}$$

with ε_0 being the permittivity of free space. The results are also shown in Table I.

II. HALL MEASUREMENTS

For the Hall measurements, a standard four-probe geometry is defined by mechanically removing the surrounding ITO film. The width and length of the Hall bars are $W = 4$ mm and $L = 30$ mm, respectively. Contacts are provided by small drops of silver paint. A constant current of 0.5 mA is applied between the source and drain contacts (A and C), and the transverse voltage $U_{B-D} = U_{AB} - U_{AD}$ is recorded using two electrometers as shown in the schematic measuring setup (Fig. 1, inset). The use of the electrometers makes it possible to investigate particle films with high resistances up to 100 GΩ and improves the signal-to-noise ratio.[19]

Figure 4 shows the result of a typical long-term measurement, taking between 30 and 60 hours. The data nicely demonstrates the problems associated with Hall measurements on samples with extremely low mobilities. Taking the common Drude expressions for the transverse and longitudinal (magneto) resistance, the ratio between the transverse and longitudinal voltages (here U_{B-D} and U_{A-C}, respectively) is equal to $\mu B \frac{W}{L}$, where μ is the mobility, B the applied magnetic field, and $\frac{W}{L}$ the aspect ratio of the Hall bar. For $\mu \approx 0.1 \frac{\text{cm}^2}{\text{Vs}}$, $B \approx 1$ T, and at $\frac{W}{L} \approx 10$ this ratio becomes $U_{B-D}/U_{A-C} \approx 10^{-6}$. Therefore even the smallest inhomogeneities or deficiencies in the sample geometry, such as imperfectly aligned Hall voltage probes, can lead to large spurious signals ($U_o \approx 45$ mV in Fig. 4) superimposed upon the Hall voltage. Furthermore, long-term fluctuations in the sample resistance (about 5% in the present case) will completely mask the influence of the magnetic field. This explains why there is very little data available regarding the Hall resistance of nanoporous materials and that most of these few articles deal with *metallic* nanoparticles.[10–13]

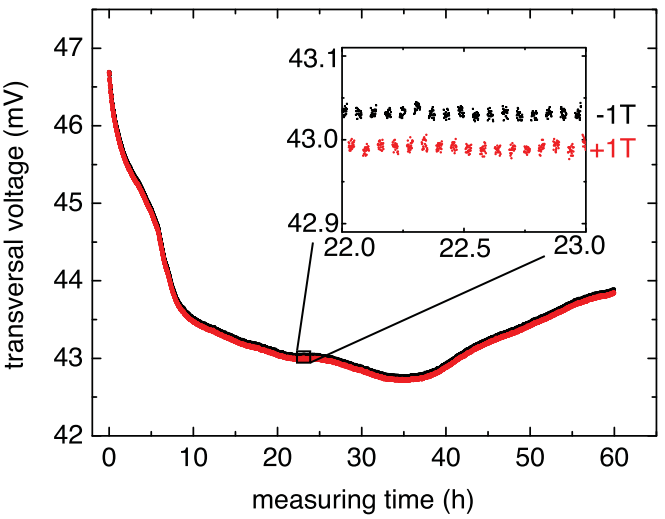

FIG. 4. (Color online) Transverse voltage measured on a Hall bar of ITO nanoparticles.

We have therefore separated out the field-induced signal by ramping B between +1 T and −1 T every 2 minutes. The small difference in the transverse voltage, induced by the oscillating magnetic field (see inset in Fig. 4), is then identified as the Hall voltage U_H and further evaluated. By using the standard formula for the Hall geometry we can calculate the carrier density n^* and mobility μ_{Hall}

$$n^* = -\frac{IB}{U_H e d} \quad \text{and} \quad \mu_{Hall} = \frac{\sigma}{ne}, \tag{7}$$

where I is the applied current and B the magnetic field.

To account for the porosity of the ITO nanoparticle layers (filling factor $f < 1$) we follow the arguments of Kharitonov and Efetov. The actual carrier concentration n_{Hall} inside the porous material, which differs from the effective carrier concentration n^*, is given by[9]

$$n_{Hall} = \frac{n^*}{A}, \tag{8}$$

with a numerical factor A determined by the shape of the particles. From the SEM characterization and the fact that $f \approx 0.79 \pm 0.05$ is only marginally larger than the filling factor of closely packed spheres, we take $A = \frac{\pi}{4}$ (spherically shaped particles[9]) to obtain the magnetotransport values for n_{Hall}.

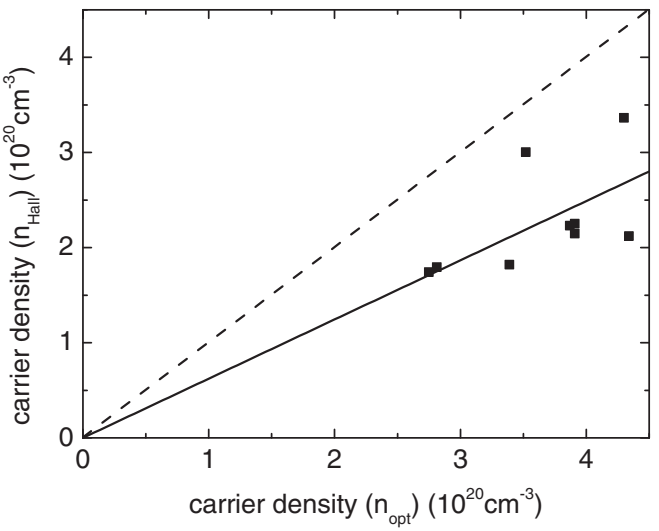

FIG. 5. Comparison of carrier concentrations obtained by optical spectroscopy (x axis) and Hall measurements (y axis). Solid line shows a linear fit of the data. Dashed line represents the identity $n_{Hall} = n_{opt}$.

III. COMPARISON AND SUMMARY

Table I shows the carrier densities and mobilities found in Hall and transmission measurements. The comparison between the carrier densities is shown in Fig. 5.

The carrier densities are of the same order as in bulk ITO. However, the values for n_{opt} are higher than for n_{Hall}. As mentioned above, we have assumed the particles to be spherical and use this assumption to calculate n_{Hall} according to Eq. (8). However, A is smaller for particles with more complex geometries, which is a possible explanation for the discrepancy between n_{opt} and n_{Hall} seen in Fig. 5.

The values for the carrier mobilities μ_{Hall} and μ_{opt} differ strongly (see Table I). In optical spectroscopy we find values about 100 times higher than in Hall measurements. This can be explained by the fact that in optical spectroscopy the carrier mobilities inside the particles are determined, which are comparable to those found in bulk ITO. This is because the mean-free path for the charge carriers is of the order of $2-3$ nm, significantly smaller than the average particle diameter, which is about 20 nm.

On the other hand, the mobility determined from magnetotransport measurements is limited by the transport across interparticle boundaries. Even in compact, microcrystalline transparent conductors, the intergrain conductivity was found to be decreased by a factor up to 10 compared to the conductivity inside the grains.[15] Experimental results[20] show that this effect should be drastically enhanced for the much smaller (nanoscale) crystals in the present study. Additionally, the porous nature of the films investigated here will further increase the macroscopic resistivity, so that a factor of 100 between optical and transport data is indeed possible.

The experimental conditions thus fulfill the requirements for granular systems described in Ref. 9 (the conductivity inside a particle was assumed to be much higher than the interparticle conductivity). In agreement with the results of Kharitonov and Efetov, we find that despite the large ratio of $\mu_{Hall}/\mu_{opt} \approx 100$, n^* can be determined with a good accuracy using the classical Hall equations, and considering a numerical factor A in the range of 0.5–1, caused by the geometry of the particles. Thus the combination of Hall measurements and optical spectroscopy is a promising way to reveal the nature of electrical conductance in nanoporous systems.

The authors gratefully acknowledge financial support by the DFG within the framework of the GRK 1240 Nanotronics.

[1] C. H. Weijtens and P. A. C. van Loon, Thin Solid Films **196**, 1 (1991).
[2] I. Hamberg and C. G. Granqvist, J. Appl. Phys. **60**, R123 (1986).
[3] J. H. Park, S. C. Lee, and P. K. Song, Met. Mater. Int. **13**, 475 (2007).
[4] N. F. Mott, *Metal Insulator Transitions* (Taylor & Francis, Ltd., London, 1974).
[5] The fundamental band gap of In_2O_3 was recently found to be 2.9 eV. A. Walsh, J. L. F. Da Silva, S.-H. Wei, C. Korber, A. Klein, L. F. J. Piper, A. DeMasi, K. E. Smith, G. Panaccione, P. Torelli, D. J. Payne, A. Bourlange, and R. G. Egdell, Phys. Rev. Lett. **100**, 167402 (2008).
[6] J. Ederth, P. Johnsson, G. A. Niklasson, A. Hoel, A. Hultaker, P. Heszler, C. G. Graqvist, A. R. van Doorn, M. J. Jongerius, and D. Burgard, Phys. Rev. B **68**, 155410 (2003).
[7] L. J. van der Pauw, Philips Res. Rep. **13**, 1 (1958).
[8] D. A. G. Bruggeman, Ann. Phys. (Leipzig) **24**, 636 (1935).
[9] M. Y. Kharitonov and K. B. Efetov, Phys. Rev. B **77**, 045116 (2008).
[10] R. K. Joshi and K. H. Sehgal, Nanotechnology **14**, 592 (2003).
[11] G. Boero, I. Utke, T. Bret, N. Quack, M. Todorova, S. Mouaziz, P. Kejik, J. Brugger, R. S. Popovic, and P. Hoffmannn, Appl. Phys. Lett. **86**, 042503 (2005).
[12] Y. Li, P. Xiong, S. von Molnar, S. Wirth, Y. Ohno, and H. Ohno, Appl. Phys. Lett. **80**, 4644 (2002).
[13] X. X. Zhang, C. Wan, H. Liu, Z. Q. Li, P. Sheng, and J. J. Lin, Phys. Rev. Lett. **86**, 5562 (2001).
[14] H. Fujiwara and M. Kondo, Phys. Rev. B **71**, 075109 (2005).
[15] I. Volintiru, M. Creatore, and M. C. M. van de Sanden, J. Appl. Phys. **103**, 033704 (2008).
[16] J. Steinhauser, S. Fay, N. Oliveira, E. Vallat-Sauvain, and C. Ballif, Appl. Phys. Lett. **90**, 142107 (2007).
[17] M. Born and E. Wolf, *Principles of Optics* (Cambridge University Press, 1959).
[18] R. Clanget, Appl. Phys. **2**, 247 (1973).
[19] Keithley Instruments, Inc., *Low Level Measurements*, 5th ed. (Cleveland, Ohio, 1998).
[20] Y. Kinemuchi, H. Nakano, M. Mikami, K. Kobayashi, K. Watari, and Y. Hotta, J. Appl. Phys. **108**, 053721 (2010).